

Numerical calculation mechanics model considering hydration of concrete

Kazuki Tajima, Kazuhito Moriizumi & Nobuaki Shirai

Department of Architecture, College of Science and Technology, Nihon University, Tokyo, Japan

ABSTRACT: A fracture mechanics model on a meso-scale level considering hydration reaction of cement is formulated and simulation results by the proposed model are presented. The proposed model is composed of three calculation routines: the hydration process on the basis of the so-called "HYMOSTRUC" developed at the Technical University of Delft, the heat conduction and thermal analyses and the numerical fracture mechanics. A unique point of this study is that a procedure identifying material parameters at an arbitrary time is developed in terms of the degree of cement hydration. Validity of the proposed procedure is investigated through applications of the thermal and cracking analyses. The present model for cracking analysis is able to clarify effect of material age on maximum load, softening curve and fracture process zone.

1 INTRODUCTION

It is an important social demand to establish not only a reliable seismic design method for concrete structures but also a design method securing long-term serviceability and maintenance system. For this purpose, it is needed to predict crack width inducing in concrete structures under various severe environmental conditions and external actions. On the other hand, to reduce environmental burdens imposed by construction activities, a various type of cement-based materials have been developed. Thus, it is expected to develop a numerical simulation procedure, which supports a rational development method of such cement-based materials.

Objective of the present study is to develop a crack simulator, which combines the meso-scale hydration model of cement-based materials with the numerical fracture mechanics model. It also can be applied for the development of new cement-based materials. In this paper, the hydration process, the thermal analysis and the numerical fracture mechanics model are outlined and then a unified calculation procedure combining these models is described. In the subsequent sections, an identification procedure used in the present study will be described and validity of the procedure will be studied through verification analyses.

2 PROPOSED MODEL

2.1 Hydration Model

The hydration reaction of cement is modeled on the basis of HYMOSTRUC developed by Breugel (1997). In most of the previous studies, it was assumed that cement particles have a single particle size in modeling the hydration reaction. However, HYMOSTRUC takes the particle size distribution defined by the following Rosin-Rammler function into consideration:

$$G(x) = 1 - \exp(-bx^n) \quad (1)$$

where $G(x)$ is the weight of cement ($G(\infty) = 1$ g); and b and n the constants.

Note that HYMOSTRUC models the interaction mechanism for particles by taking the particle size distribution of cement into consideration. Figure 1 shows the interaction mechanism for particles schematically. In the hydration process, state of cement particles can be classified into three categories; the unhydrated cement, the inner product and the outer product. With the development of hydration, expanding particles embed surrounding small particles into theirs and further expand by their embedded amount.

It is important to model an interaction between the microstructure development stated in the above and the hydration rate. For this, the size distribution and the spatial distribution of particles must be evaluated adequately. In HYMOSTRUC, the spatial distribution of particles is defined as a cube space, which is referred to as the "cell" as shown in Figure.2.

2.2 Numerical Fracture Mechanics Model

The numerical fracture mechanics model is a calculation procedure, which utilizes the meso-scale particle model for simulating crack development and the heat conduction and thermal stress analyses by the finite element method. The present particle model is based on the method proposed by Jirasek and Bazant(1994/1995,1995) and is summarized as follows(Moriizumi and Shirai, 1998):

1. A lattice network is constructed with link elements which transmit only axial force.
2. Nonlinear stress-strain relation including tension softening behavior is assigned to each link (see Fig.3).
3. The method of inelastic forces is applied to solve nonlinear equations.

Jirasek and Bazant constructed the particle model without considering the multi-phase structure inside concrete. On the other hand, the present study defines the lattice network consisting of three phases; the mortar, coarse aggregate and interface links (see Fig.4). Microscopic material properties are provided for each link by assuming that cracking is only al-

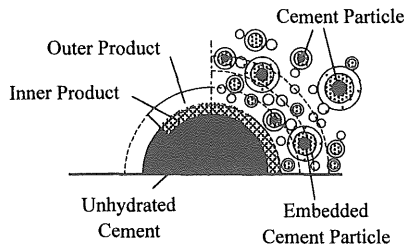


Figure 1. Interaction mechanism for particles

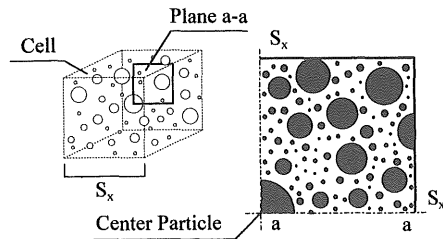


Figure 2. Definition of Cell

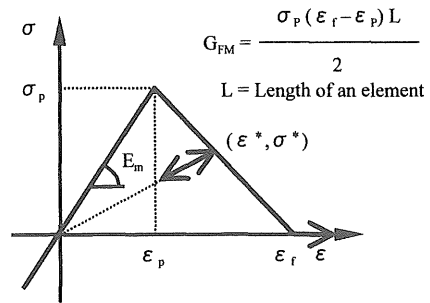


Figure 3. Microscopic stress-strain relation

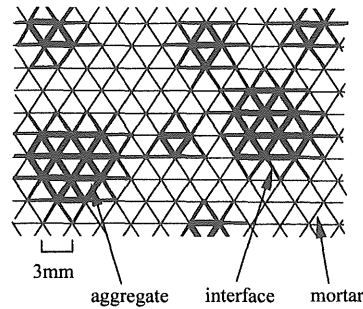


Figure 4. Particle model of three-component material

lowed to occur in the mortar links, and the coarse aggregate links are treated as the elastic material.

Moriizumi & Shirai (1998) derived a relationship between microscopic parameters of mortar and the macroscopic responses obtained through the parametric study on the mortar prismatic specimens under tensile stress by the particle model.

2.3 Unified Calculation Procedure with Proposed Model

First, development in material properties of the cement matrix is evaluated, and then its information is provided for the numerical fracture mechanics model. Finally, the model for simulating micro-cracking behaviors developing through the cement matrix is formulated. The calculation flowchart is shown in Fig.5.

2.3.1 Hydration analysis

The calculation of hydration process and the heat conduction and thermal stress analyses are conducted in the time domain. In HYMOSTRUC, the penetration depth of each cement particle $\delta_{m;x,j+1}$ is calculated based on the cement composition, the size distribution and the water-cement ratio by the basic rate equation as:

$$\frac{\Delta \delta_{m;x,j+1}}{\Delta t_{j+1}} = \frac{K_i F_1 F_2^\lambda \Omega_1 \Omega_2 \Omega_3}{\left\{ (\delta_{x,j})^\lambda \right\}_j} \quad (2)$$

where Δt_{j+1} is the time increment; $\delta_{m;x,j+1}$ the increase of penetration depth of particle with diameter x during Δt_{j+1} ; K_i the reaction rate constant (the phase-boundary reaction for $i = 0$ and the diffusion-controlled reaction for $i = 1$); F_1 and F_2 the temperature functions accounting for the effect of curing temperature; Ω_1 , Ω_2 and Ω_3 the reduction factors accounting for the effect of water state; $\delta_{x,j}$ the total thickness of product layer of particle with diameter x at the end of the time step Δt_{j+1} ; λ the factor indicating the phase-boundary reaction for $\lambda = 0$ and the diffusion-controlled reaction for $\lambda = 1$; and β_1 the constant.

The degree of hydration α_x can be determined by the equation as (HYMOSTRUC):

$$\alpha_x = 1 - \left\{ 1 - \left(\frac{\delta_{m;x,j}}{r_0} \right) \right\}^3 \quad (3)$$

where α_x is the degree of hydration of each particle; $\delta_{m;x,j}$ the penetration depth; and r_0 the particle size of cement.

The overall degree of cement hydration α can be determined with the degree of hydration of each particle α_x . The temperature rise in the cement paste ΔT_j can be calculated by the equation as (HYMOSTRUC):

$$\Delta T_j = \frac{\alpha_j Q^{\max} G_c}{\rho_c c_c} \quad (4)$$

where α is the overall degree of hydration; Q^{\max} the maximum heat of hydration; G_c the cement content in the mix; ρ_c the specific mass of the sample; and c_c the specific heat of the sample.

The quantities defined in the above are evaluated at the nodal points of finite elements used in the heat conduction and thermal analyses, and the resulting degree of hydration α and temperature in the cement paste T are utilized as the input data for the numerical fracture mechanics model.

The degree of hydration α obtained by the hydration reaction model has to be related to the characteristic value of heat for the heat conduction and thermal stress analyses and the microscopic material properties for the cracking analysis by the particle model. The identification study of material properties will be discussed in § 3.

2.3.2 Heat Conduction and Thermal stress analyses

The heat conduction analysis by FEM is carried out using the temperature of cement paste and the exter-

nal temperature. Then, the thermal stress distribution in the specimen can be calculated by conducting the thermal stress analysis of the specimen under the resulting temperature distribution and the given boundary condition.

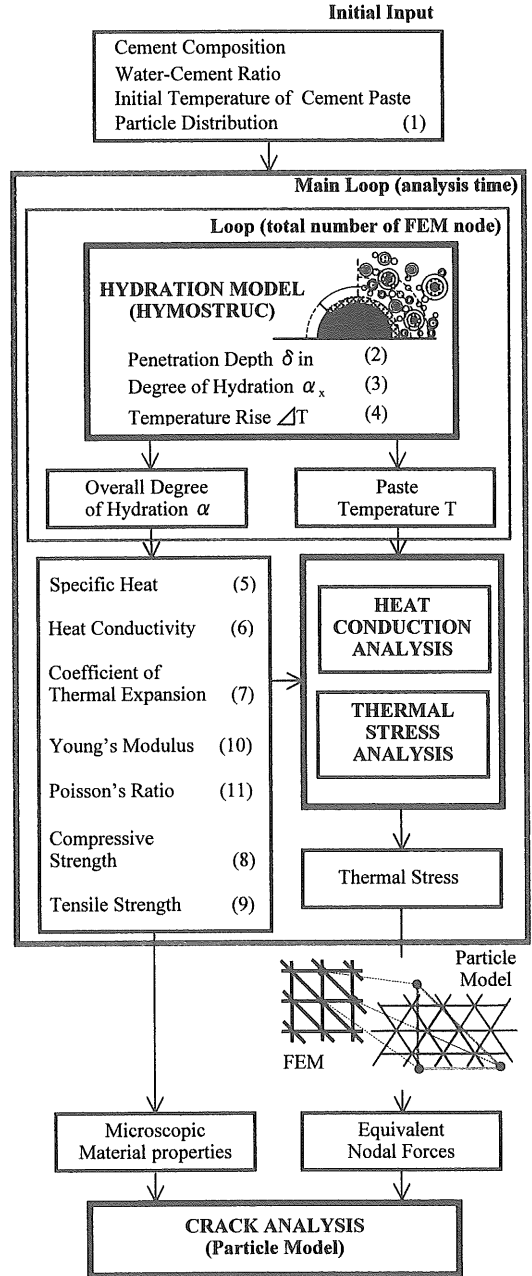


Figure 5. Calculation Flowchart

2.3.3 Model for cracking analysis.

The cracking analysis with the particle model shall be carried out not in the time domain but at a certain target time; that is, the thermal stress created until a target time is used as an initial stress for the cracking analysis. For this purpose, the thermal stress in an element is transformed into the equivalent nodal forces and they are applied to the corresponding nodal points of link network as a set of initial load. Finally, the cracking analysis of specimen is conducted under increasing external forces, and the crack development and fracture energy are evaluated.

3 MATERIAL PARAMETERS

Since material properties of cement vary with the development of hydration, they have to be expressed in terms of time. The material parameters used in the present analysis are the characteristic values for the heat conduction and thermal stress analyses and the microscopic material properties in the particle model, and they are determined using the degree of hydration.

3.1 Characteristic values of heat

The thermal conductivity, the specific heat and the coefficient of thermal expansion are taken into account as the characteristic values of heat for the heat conduction and thermal stress analyses.

3.1.1 Heat conductivity

According to RILEM report (1981), the thermal diffusivity is almost constant during the ages from 1 to 7 days. It is also known that the thermal diffusivity gives a similar tendency to the heat conductivity. Thus, assuming that the heat conductivity would not change with time, it is calculated by the equation as (Comphbell-Allen & Thoren 1963):

$$\lambda = \frac{2\lambda_p + \lambda_a - 2V_a(\lambda_p - \lambda_a)}{2\lambda_p + \lambda_a + V_a(\lambda_p - \lambda_a)} \lambda_p \quad (5)$$

where λ_p is the heat conductivity of cement paste; λ_a the heat conductivity of aggregate; and V_a the aggregate content of the mix. Now, the effect of aggregate on the heat conductivity of concrete has been considered in Eq. (5).

3.1.2 Specific heat

The specific heat of water is about 5 times of specific heat of unhydrated cement and aggregate. For this reason, the specific heat of concrete becomes higher with the increase in water content and decreases with the progression of drying. In this study, the specific heat of concrete is calculated by the equation expressed in terms the degree of hydration as (Tomozawa et al. 1996):

$$c_c = \frac{1}{W + Ce + S + G} \frac{1}{(4.186W + 0.904Ce + 0.796S + 0.771G) (1 - \alpha) + 1.17\alpha} \quad (6)$$

where W , Ce , S and G are the contents of water, cement and fine and coarse aggregate, respectively.

3.1.3 Coefficient of thermal expansion

The coefficient of thermal expansion in concrete varies significantly in the early age. In this study, a relationship between the coefficient of thermal expansion and the degree of hydration is derived with reference to the previous test results on the coefficient of thermal expansion for early age concrete (Shimasaki & Rokugo 2000). Figure 6 shows the relationship between the average values of measured coefficients of thermal expansion, and an identified relation can be written in terms of the degree of hydration as:

$$\begin{aligned} \zeta &= 20.35 \times 10^{-6} \exp(-1.674\alpha) \quad (\alpha \leq 0.6) \\ \zeta &= 8.0 \times 10^{-6} \quad (\alpha > 0.6) \end{aligned} \quad (7)$$

There is a large amount of water of unhydrated state in the initial hardening process of concrete. Thus, the coefficient of thermal expansion of concrete strongly depends on water with larger coefficient of thermal expansion than cement or aggregate. As a result, the coefficient of thermal expansion becomes larger in a very early stage of hardening. To deal with such phenomena, the coefficient of thermal expansion is approximated by two kind of equations.

3.2 Microscopic material properties

Material parameters considered in the particle model are the microscopic tensile strength σ_p and the limit strain ε_f . Moriizumi et al. (1998) derived the relationship between these microscopic parameters and the macroscopic parameters as described below. The macro-fracture energy of mortar G_F can be related to the micro-fracture energy G_{FM} as:

$$G_F = 1.35G_{FM} \quad (8)$$

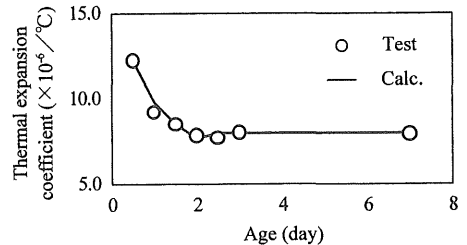


Figure 6. Thermal expansion coefficient and age

G_{FM} in Eq.(8) can be obtained by the equation as:

$$G_{FM} = \frac{\sigma_p(\varepsilon_f - \varepsilon_p)L}{2} \quad (9)$$

where L is the length of a link element. Since ε_p is sufficiently small in comparison with ε_f , ε_p shall be neglected in this study. Next, the macroscopic tensile strength f_i can be related to the microscopic material parameters as:

$$f_i = 0.67\sigma_p + 31.83\varepsilon_f + 0.43 \quad (10)$$

The quadratic equation with respect σ_p including f_i and G_{FM} can be derived combining Eqs. (8) to (10). Finally, the microscopic parameters can be determined in terms of such macroscopic material parameters as f_i and G_F by solving the equation.

3.2.1 Macroscopic strength & Young's modulus

Schutter (1996) derived the relationship between the degree of hydration and the compressive strength of concrete as follows:

$$\frac{f_c(\alpha)}{f_c(\alpha=1)} = \left(\frac{\alpha - \alpha_0}{1 - \alpha_0} \right)^a \quad (11)$$

where $F_c(\alpha)$ is the compressive strength of concrete at α ; and α_0 the constant.

The compressive strength is determined from Eq. (11) in this study. Then, the tensile strength of concrete f_{cm} can be calculated from the formula in terms of the compressive strength of concrete recommended in the CEB-FIP Model Code 1970 written as:

$$f_t = 0.28(f_c)^{2/3} \quad (12)$$

where f_c is the compressive strength of concrete.

In addition, Schutter (1996) derived the equations describing Young's modulus and Poisson's ratio in terms of the degree of hydration as follows:

$$\frac{E_{co}(\alpha)}{E_{co}(\alpha=1)} = \left(\frac{\alpha - \alpha_0}{1 - \alpha_0} \right)^b \quad (13)$$

where $E_{co}(\alpha)$ is Young's modulus at α ; and α_0 and b the constants.

$$\nu(\alpha) = 0.18 \sin \pi\alpha / 2 + 0.5 \times 10^{-10\alpha} \quad (13)$$

where $\nu(\alpha)$ is Poisson's ratio at α .

3.2.2 Macroscopic fracture energy

The fracture energy of concrete can be calculated by the formula recommended in the CEB-FIP Model Code (1990) expressed in terms of the compressive strength of concrete and the maximum size of coarse aggregate as :

$$G_F = \alpha_f \left(\frac{f_{cm}}{f_{cm0}} \right)^{0.7} \quad (14-1)$$

$$\alpha_f = 0.00125 d_{max} + 0.01 \quad (14-2)$$

where f_{cm} is the compressive strength of concrete; $f_{cm0} = 10$ MPa, and d_{max} the maximum size of aggregate.

3.2.3 Identification of microscopic material parameters

The microscopic material parameters have to be determined for conducting the cracking analysis with the particle model. However, it must be noticed that Eqs. (11), (12) and (14) give the macroscopic compressive and tensile strengths and fracture energy of concrete. Now, it is needed to determine the microscopic material parameters. First, the microscopic material parameters of concrete are calculated by Eqs. (8), (9) and (10) using the tensile strength and the fracture energy of concrete. Now, it must be noted that G_F in Eq. (8) is the macro-fracture energy of mortar. However, there is no reliable formula for determining G_F of mortar. So, it is extrapolated from G_F in Eq. (14) for concrete according to the following procedure. First, assuming the maximum size of fine aggregate, the macro-fracture energy of mortar is calculated by Eq. (14), and the ratio of the fracture energy for mortar to that for concrete is calculated. Then, the values of microscopic parameters are determined by multiplying the values of microscopic parameters of concrete with the ratio in the above.

4 VERIFICATION ANALYSIS

In order to study validity of the material parameters to be calculated by the procedure stated in the previous section, the verification analysis is conducted on concrete specimen.

4.1 Temperature Analysis

To study validity of the procedure for identifying thermal characteristic values, temperature distribution in the specimen is calculated by the proposed model. The specimen to be analyzed is a square massive concrete specimen with size of 2x2x2 m³ tested by Suzuki (1990).

The geometry of specimen is shown in Fig.7. The specimen was cured under the semi-adiabatic condition: that is, the specimen was covered with the styrene foam with thickness of 100 mm.

The composition of cement and the mix proportion of concrete are listed in Tables 1 and 2, respectively. Note that temperature distribution at the surfaces and inside of the specimen was calculated by assuming that all surfaces of the specimen were under the heat transmission boundaries.

Figure 8 compares the predicted results with the observed ones. Although the analysis tends to over-estimate a slope of temperature rise in comparison with the observed one in the early stage, the predicted values are relatively in good agreement with the observed ones. The predicted distributions of temperature and principal stresses are shown in Fig.9.

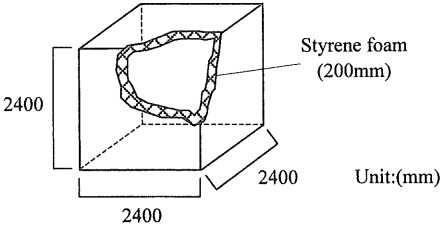


Figure 7. Geometry of specimen

Table 1. Cement composition

| C ₃ S | C ₂ S | C ₃ A | C ₄ AF | unit (%) |
|------------------|------------------|------------------|-------------------|----------|
| 47.2 | 27.4 | 10.4 | 9.4 | |

Table 2. Mix proportion

| w/c | s/a (%) | Unit Contents (kg/m ³) | | | |
|------|---------|------------------------------------|-----|-----|------|
| | | W | Ce | S | G |
| 0.75 | 42.1 | 158 | 212 | 812 | 1118 |

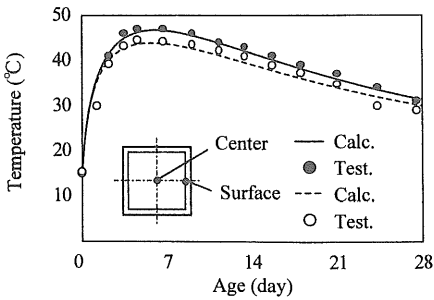


Figure 8. Temperature history of concrete specimen

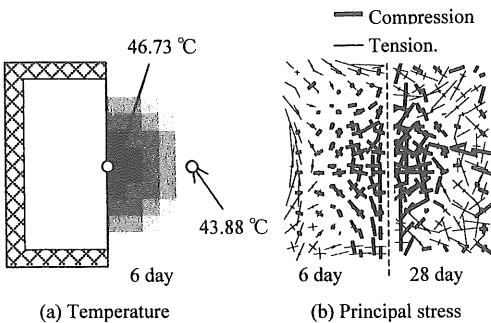


Figure 9. Distribution of temperature and principal stress

4.2 Verification of material parameters

Validity of the relationship between the macroscopic parameters and the microscopic parameters derived in the previous section is investigated by conducting the cracking analysis on concrete specimens.

The specimens analyzed are 3-point bend beams with a single notch made of normal concrete tested by Rokugo et al. (1991). Figure 10 shows the geometry of specimens. The test was performed at the different ages of 3, 7 and 28 days. The specimens were cured under the moisture condition until a day before the test. Since the composition of cement and the mix proportion have not been given in the literature, typical values of the material parameters for normal concrete are assumed. Tables 3 and 4 give the composition of cement and the mix proportion of concrete, respectively. Table 5 indicates the test results of material properties. Note that Young's modulus of concrete is calculated by the formula of AIJ code (1988) using the specific mass and the compressive strength of concrete.

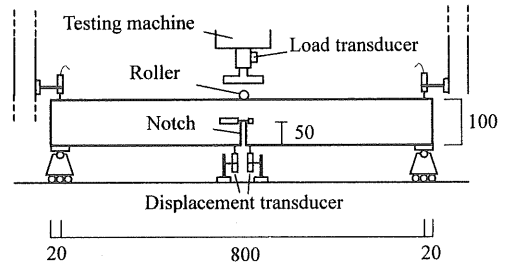


Figure 10. 3-point bending test on notched beam by Rokugo

Table 3. Cement composition

| C ₃ S | C ₂ S | C ₃ A | C ₄ AF | unit (%) |
|------------------|------------------|------------------|-------------------|----------|
| 50.0 | 25.0 | 9.0 | 9.0 | |

Table 4. Mix proportion

| w/c | s/a (%) | Unit Contents (kg/m ³) | | | |
|------|---------|------------------------------------|-----|-----|-----|
| | | W | Ce | S | G |
| 0.53 | 48.0 | 180 | 340 | 876 | 949 |

$d_{max} = 15 \text{ mm}$

Table 5. Test result of material properties

| Age (day) | Comp. Strength (MPa) | Tens. Strength (MPa) | Flex. Strength (MPa) | Young's Modulus (Mpa) |
|-----------|----------------------|----------------------|----------------------|-----------------------|
| 3 | 19.1 | 1.73 | 3.75 | 20920 |
| 7 | 28.6 | 2.62 | 4.57 | 25603 |
| 28 | 39.9 | 3.36 | 4.95 | 30224 |

The parameters used in the analysis are also listed in Table 6. These parameters were so determined that the calculated compressive strength and Young's modulus of concrete at the age of 7 or 28 days would fit to the corresponding test results.

Figure 11 shows the comparison between the predicted and observed results at the different ages. Figures 11 (a)-(c) show the comparison between the predicted and observed results at each age, and Fig.11 (d) shows the comparison of predicted results. It is seen that the predicted curves after the peaks fall in the observed bands. The microscopic parameters in the present analysis were determined on the basis of the macroscopic compressive strength at the age of 7 or 28 days. Although the analysis gives a little bit higher maximum loads than observed ones, overall agreement is reasonably good. In addition, the analysis can simulate the tendency with reasonable accuracy that the maximum load increases with a variation of material age and the slope of softening curve after the peak becomes steeper.

Now, let us discuss the crack development at each age. Figure 12 shows the cracking patterns near the notch obtained at each age. The cracking patterns shown correspond to those at the maximum loads, those at which the center displacement reached 5 and 10 mm, and those at the final stage. The common tendency observed in all cases is that the fracture process zone becomes narrower with the increase in age. The hydration of cement is still active during young ages, and thus concrete is still in the process that the generation of microstructure is developing. This indicates that the development of strength and Young's modulus is not mature. Consequently, it seems that cracking occurred in a wide range of the specimen even at low stress levels. On the other hand, in the case of higher ages, the hydration of cement is advanced, the microstructure of concrete is sufficiently generated, and the values of strength and Young's modulus are sufficiently enhanced. Thus, it seems that cracking does not occur until stresses induced in the specimen increase up to the tensile strength developed, and thus cracking localizes to a narrower range.

According to the predicted crack patterns, cracking did not occur until the maximum loads for both specimens of each age. When the center displacement of specimen reached 5 mm, cracking initiated near the notch and a number of link elements in either the softening or unloading branch significantly increased in the specimens for both ages. Now, when the center displacement reached 10 mm, cracking almost progressed to the final cracking state. The slope of softening curve predicted by the analysis changes when the center displacement reached 5 mm. It seems that most of cracks have occurred in the specimen until the moment at which

the center displacement reaches 5 mm after the peak load. In addition, in case of the specimens for age of 3 or 7 days, curved cracking lines penetrating through around aggregates are generated. On the

Table 6. Parametric value

| α_0 | $f_c (\alpha=1)$ (MPa) | a | $E_{co} (\alpha=1)$ (MPa) | b |
|------------|---------------------------|------|------------------------------|------|
| 0.25 | 43.6 | 1.21 | 31589 | 0.61 |

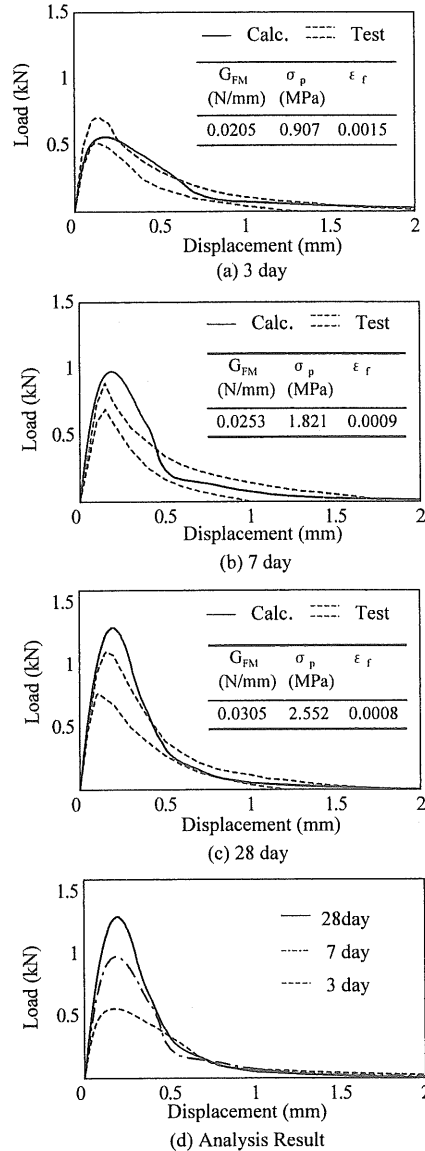


Figure 10. Load-Displacement curves

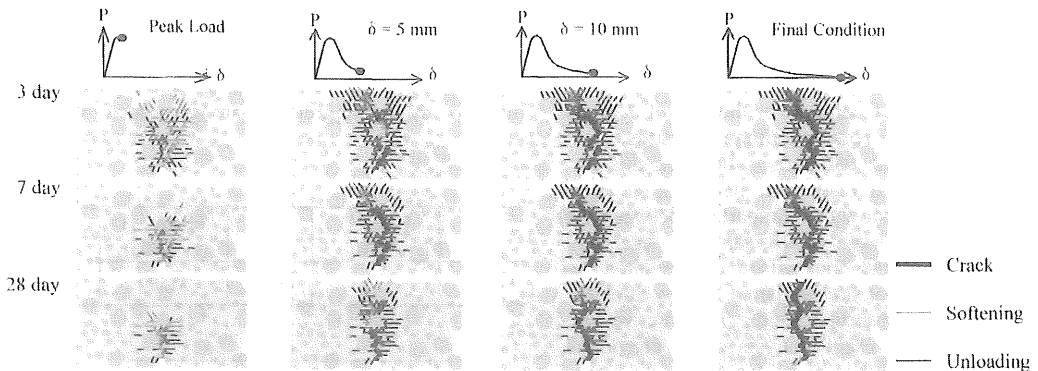


Figure 12. Crack analysis Result

other hand, in case of the specimen for age of 28 days, less curved cracking lines are generated, and localization of the fracture process zone becomes noticeable

5 CONCLUSION

The numerical fracture mechanics model considering the hydration reaction is formulated, and the variable material parameters with the development of hydration are identified. The following results are obtained through the verification studies:

1. The material parameters used in the analysis are determined on the basis of the degree of hydration, and it was verified that the procedure for identifying the material parameters is reasonably acceptable.
2. Although the thermal analysis tends to overestimate the slope of temperature rise in comparison with the observed one in the early stage, the predicted values are relatively in good agreement with the observed ones.
3. Although the cracking analysis with the proposed model tends to overestimate the maximum load slightly, it is able to simulate the effect of material age on the maximum load, the softening curve and the fracture process zone.
4. It is strongly recommended that further experimental tests will be conducted to establish a reliable procedure for determining material parameters.

ACKNOWLEDGEMENT

This research was conducted as a part of the Academically Promoted Frontier Research Program on "Sustainable City Based on Environmental Preservation and Disaster Prevention" at Nihon University, College of Science and Technology (Head Investigator: Prof. Nagakatsu Kawahata) under A Grant from the Ministry of Education, Science, Sports and Culture and was partially supported by Japan Society for the Promotion of Science under Grant-in-Aid for Scientific Research (C).

REFERENCES

- Breugel, K. van. 1997. Simulation of hydration and formation structure in hardening cement-based material. *PhD thesis*, Delft University of Technology.
- Jirasek, M. & Bazant, Z.P. 1994/1995. Macroscopic fracture characteristics of random particle systems. *International Journal of Fracture* Vol.69: 201-228.
- Jirasek, M. & Bazant, Z.P. 1995. Particle model for quasibrittle fracture and application to sea ice. *Journal of Engineering Mechanics*: 1016-1025.
- Morizumi, K., Shirai, N. & Suga, H. 1998. Fracture and softening analysis of concrete with particle model. *Proc. of FRAMCOS-3* Vol.2: 931-938. AEDIFICATIO Pub.
- Commission 42-CEA, RILEM. 1981. Properties of set concrete at early ages state-of-the-art report, *Material and Structures* Vol.14 No.84: 399-450.
- Comphbell-Allen, D. & Thoren, C.P. 1963. The thermal conductivity of concrete, *Magazine of concrete research* Vol.15 No.43.
- Tomozawa, F., Noguchi, T. & Hyeon, C. 1996. Study on cement hydration model prediction of temperature in concrete by hydration model of cement.; *Proc. of JCI symp.*, Japan: 13-20.
- Shimasaki, I., Rokugo, K. & Morimot, H. 2000. On thermal expansion coefficient of concrete at very early ages. *International workshop on control of cracking in early-age concrete*, Sendai, Japan: 49-56.
- De Schutter, G., Taerwe, L. 1996. Degree of hydration-based description of mechanical properties of early age concrete. *Materials and Structure* Vol.29: 335-344.
- CEB-FIP. 1970. Recommendations internationales pour le calcul et l'execution des ouvrages en beton,
- CEB-FIP. 1990. Model Code 1990 Final Draft, Bulletin d'information.
- Suzuki, Y. 1990. Heat of hydration evolution process of cement in concrete and quantification. *PhD thesis*, University of Tokyo.
- Rokugo, K., Uchida, Y. & Koyanagi, W. 1991. Fracture energy and tension softening diagrams of various kinds of concrete. *Brittle Matrix Composites* Vol.3, Elsevier applied science: 101-110.
- AIJ. 1988. Standard for structure calculation of reinforced concrete structure. Japan.